OPEN ACCESS

International
Journal
Of Modern Engineering Research (IJMER)

Slow-fast oscillations in a periodically excited symmetric chaotic oscillator with multiple time scales

Yandan Jiang, Junting Gou, Zhengdi Zhang, Qinsheng Bi*
Faculty of Science, Jiangsu University, Zhenjiang Jiangsu 212013, PR China

Abstract:
The dynamics of the autonomous systems with multiple time scales can be explored by the geometric singular perturbation theory, which however cannot be used to investigate the mechanism of the relaxation oscillations in non-autonomous oscillators. For the periodic excited systems, when the exciting frequency is far less than the natural frequency, which implies the coupling of two time scales in frequency involves the dynamics, relaxation oscillations, called also the bursting oscillations, can often be observed. Here we refer to the geometric singular perturbation theory, and propose a method to reveal the mechanism of the behaviors of periodically excited vector fields. Furthermore, for a symmetric system with the coupling of different time scales, multi-stability may lead to more complicated behaviors when the slow-varying periodic excitation is introduced. Here we consider a typical chaotic oscillator with slow-varying external excitation. With the variation of the exciting amplitude, different types of bursting oscillations are presented, the mechanism of which is explored by the proposed method. It is found that, the multi-stability in the system can not only lead to different attractors, but also cause the dynamics to alternate between a symmetric attractor and a pair of coexisted asymmetric attractors, depending on the particular attracting basins of the stable equilibrium branches the trajectory visits.

Date of Submission: 11-03-2021 Date of acceptance: 26-03-2021

I. INTRODUCTION

The coupling of different scales can be found in many mathematical models in science and engineering problems [1], which may often cause the relaxation oscillations, called also bursting oscillations, characterised by the combination of large-amplitude oscillations (spiking states, SPs) and small-amplitude oscillations or at rest (quiescent states, QSs) [2]. The earliest work may date back to discovery of the relaxation oscillations of singular Van der Pol equation at the end of 19th century [3]. However, it was until the Hodgkin-Huxley model was established, the slow-fast dynamics receives much attention, since the H-H model can exhibit the bursting activities in neurons [4].

Since no valid analytical method exists to explore the interaction between different scales [5], in the first stage of the related study, researchers focused on the approximated solutions and presented a few approaches, such as the quasi-steady state method and singular perturbation method [6].

Oscillations with clearly separated amplitudes have been observed in many application areas [7]. How to explain the transitions between them becomes one of the hot topics in the systems with multiple time scales [8]. Dynamical system theory studies qualitative properties of the solutions of differential equations, especially the bifurcations of equilibria and periodic orbits [9]. Bursting oscillations may be periodic orbit, but we then ask the questions that how can we apply the dynamical system theory to reveal the transitions. Beginning with the work of Takens on constrained vector field [10], geometric methods have been used to study the generic multiple-time-scale systems with slow and fast state variables [11]. Fenichel's seminal work on invariant manifolds was an initial foundation of the geometric singular perturbation theory [12], which takes a geometric point of view and focuses on invariant manifolds, normal forms for singularities, and analysis of their unfoldings [13].

The main idea of geometric singular perturbation theory is to consider the behaviors of slow and fast subsystem separately, in which a typical autonomous slow-fast system can be expressed in the form [14]

$$\begin{aligned} \dot{x} &= f(x, y, \mu), \quad \text{(Fast Subsystem)} \\ \dot{y} &= \varepsilon g(x, y, \mu), \quad \text{(Slow Subsystem)} \end{aligned} \tag{1}$$

where $x \in R^M, y \in R^N, \mu \in R^K$, while $0 < \varepsilon \ll 1$ describes the ratio between the fast and slow scales. The functions f, g are assumed to be sufficiently smooth. The state variables x are fast and the variables y are slow.

As $\varepsilon \to 0$, the trajectories of (1) converge during the fast epochs to the solution of the fast subsystem [15]

$$\begin{aligned} \dot{x} &= f(x, y, \mu), \\ \dot{y} &= 0, \end{aligned}$$

(2)

During slow epochs, on the other hand, the trajectories of (1) converge to the solution of

$$\begin{aligned} 0 &= f(x, y, \mu), \\ \dot{y} &= \varepsilon g(x, y, \mu), \end{aligned}$$

(3)

which is differential-algebraic equation called the slow flow or reduced system [16]. One goal of Geo-metric singular perturbation theory is to use the fast and slow subsystems (2) and (3) to understand the dynamics of the full system (1). The algebraic equation in (3) defines the critical manifold [17]

$$S := \left\{ (x, y) \in R^m \times R^n \,\middle|\, f(x, y, \mu) = 0 \right\},$$

(4)

the points of which are equilibrium points for the fast subsystem. By the characteristic analysis of the equilibrium points of the fast subsystem, the branch S can be divided into three types of subsets, corresponding to repelling, attracting and saddle types, respectively [18]. Hyperbolicity of the fast subsystem fails at the points on S where its projections onto the space of slow variables is singular. From the implicit function theorem, equilibrium branch S implies $y = h(x)$. Therefore, the behaviors of the trajectory at the singular points on S may be described by [19]

$$\dot{x} = \varepsilon (D_x h(x))^{-1} g\left[x, h(x), \mu\right].$$

(5)

By regarding the slow state variables y as slow-varying parameters, the equilibrium branches as well as their bifurcations of the fast subsystem with the variation of y can be derived. The mechanism of the bursting oscillations can then be obtained by overlapping the phase portrait and equilibrium branches on the (x, y) plane [20], in which the fast subsystem can be used to determine the quiescent states and the spiking states and the bifurcations at the alternations, while the slow subsystem can be employed to investigate the modulation by the slow process [21].

Many types of bursting attractors and their mechanism have been reported by the geometric singular perturbation theory, which can be classified by the structures, such as point-cycle, cycle-cycle bursting attractors [22], or by the related bifurcations, for example, the fold-fold, fold-Hopf bursting attractors [23]. However, most of the results are obtained based on autonomous slow-fast systems, while the bifurcations at the transitions are commonly codimension-one bifurcations [24]. For periodically excited dynamical systems, when the exciting frequency is far less than the natural frequency, relaxation oscillations can also be observed, how to explore the mechanism of such bursting attractors is still an open problem [25]. Meanwhile, when the multi-stability involves the vector fields, the bifurcations may lead to a set of behaviors, which therefore result in different forms of bursting oscillations, seeing the bursting attractor with cusp bifurcation [26].

Here we proposed a method to explore the mechanism of bursting oscillations in periodically excited dynamical systems. The method is then used to analyze the dynamical evolution of a para-metrically excited vector field with pitchfork-Hopf bifurcation.

II. SLOW-FAST ANALYSIS METHOD FOR TWO SCALES IN FREQUENCY DOMAIN

Here we consider periodically excited system, written in the form

$$\dot{x} = f\left[x, \mu, A\sin(\varepsilon\Omega t)\right], \tag{6}$$

where $x \in R^M, y \in R^N, \mu \in R^K$, while $0 < \varepsilon \ll 1$. Two scales in frequency exist, corresponding to the natural frequency and the exciting frequency, respectively. Since no obvious slow and fast subsystems can be defined, new method need to be developed to investigate the mechanism of the dynamics. For the purpose, we refer to the geometric singular perturbation theory and rewrite (6) as

$$\begin{aligned} \dot{x} &= f(x,\mu,w), \quad (\text{Fast Subsystem}) \\ w &= A\sin(\varepsilon\Omega t), \quad (\text{Slow Subsystem}) \end{aligned} \tag{7}$$

Generalize autonomous system. Similar to the method by Rinzel, we regard the whole exciting term w as a generalized slow state variable, like y in (1). The fast subsystem is then expressed in the generalized autonomous system, while the slow subsystem is described by a slow-varying function of time.
The critical manifold is defined as

$$S := \left\{(x,w) \in R^m \times R \,\middle|\, f(x,\mu,w) = 0\right\}, \tag{8}$$

the points of which are equilibrium points for the fast subsystem. We call a normally hyperbolic subset $M \subset S$ attracting if all eigenvalues of $(D_x f)(p,u)$ have negative real parts for $p \in M$; similarly, M is called repelling if all eigenvalues have positive real parts. If M is normally hyperbolic and neither attracting nor repelling, we say it is of saddle type.
Away from the singular points on the S, the implicit function theorem implies that S is locally graph of a function $w = h(x)$, which leads to $D_x h(x)\dot{x} = \varepsilon\Omega A\cos(\varepsilon\Omega t) = \pm\varepsilon\Omega\sqrt{A^2 - w^2}$. Therefore, the behaviors of the trajectory at the singular points on S may be described by

$$\dot{x} = \pm\varepsilon\Omega\left[A^2 - h(x)^2\right](D_x h(x))^{-1}. \tag{9}$$

For the fixed parameters μ, we can derive not only the equilibrium branch $x = v(w)$, but also the bifurcation points $p^*(x^*, w^*) \in S$.

Transformed phase portrait. Since the equilibrium branch and the dynamics of the fast generalized autonomous system may change with the variation of w, here we introduce the conception of the transformed phase portrait, defined by $\Pi_G \equiv \left[(x,w)\middle|t \in R\right] = \left\{\left[x, A\sin(\Omega t)\right]\middle|t \in R\right\}$, in which w is regarded as a generalized state variable, like y in (1).
The corresponding relationship between the proposed method and the geometric singular perturbation theory is listed in Table 1.
The overlap of the phase portrait and the equilibrium branches on the (y,x) plane can be used to reveal the mechanism of the bursting oscillations in autonomous slow-fast systems. Accordingly, regarding w as a generalized state variable, we can find the mechanism of the bursting oscillations in non-autonomous systems with slow-varying periodic excitations by overlapping the transformed phase portrait and the equilibrium branches and their bifurcations of the fast subsystem with the variation of the slow-varying parameter w. Based on the method, serval types of bursting oscillations and their mechanism with codimension-1 bifurcations in parametrically or externally excited systems is presented, which exhibits quite difference comparing with the bursting oscillations in autonomous systems [27].
In the following, we focus on the effect of two scales in the frequency domain on the dynamics of a modified symmetric $R\ddot{o}ssler$ system by introducing a slow-varying periodic excitation to investigate the influence of multi-stability on the bursting evolution. Several new types of bursting oscillations exhibiting a few special interesting phenomena are obtained, the mechanism of which is presented by the proposed method.

Table 1: Comparison between the proposed method and the geometric singular perturbation theory

	Geometric singular perturbation theory	Proposed method
Fast subsystem	$\dot{x} = f(x,y,\mu)$	$\dot{x} = f(x,w,\mu)$
Slow subsystem	$\dot{y} = \varepsilon g(x,y,\mu),$	$w = A\sin(\varepsilon\Omega t)$
Slow variable	y	w
Critical manifold	$f(x,y,\mu) = 0$	$f(x,w,\mu) = 0$
Reduced equation	$\dot{x} = \varepsilon(D_x h(x))^{-1} g[x,h(x),\mu)]$	$\dot{x} = \pm\varepsilon\Omega\left[A^2 - h(x)^2\right](D_x h(x))^{-1}$
Equilibrium branch	$x = h(y,\mu)$	$x = h(w,\mu)$
Phase portrait	(y,x)	(w,x)

III. MATHEMATICAL MODEL

Unlike many famous symmetric chaotic systems such as Lorenz oscillator [28] and Chen's system[29], the chaotic $R\ddot{o}ssler$ system with multi-stability is asymmetric, since only quadratic nonlinear terms exist, which can be modified to appear in the symmetric form [30],

$$dx/dt = -y - yz,$$
$$dy/dt = x + ay + w,$$
$$dz/dt = b + z(hx^2 - c),$$

(10)

where $w = A\sin(\varepsilon\Omega t)$ represents the external periodic excitation.

When $A = 0$, the multi-stability in the symmetric system may lead to the strange attractor oscillating around different stable equilibrium points [31]. When $A \neq 0, \varepsilon = 1,$ for a regular Ω value, the dynamics may evolve from limit cycle to chaotic oscillations via sequence of period-doubling bifurcations [32]. However, when $0 \ll \varepsilon \ll 1$, implying the coupling of two scales in frequency domain exists, bursting oscillations may appear observed, characterised by the combination of large- amplitude oscillations, called the repetitive spiking state (SP), and the small-amplitude oscillations or at rest, represented by the quiescent state (QS).

Obviously, the vector field still keeps its symmetry since it remains unchanged with the transformations $(x, y, z, t) \to (-x, -y, z, t + \pi/\Omega)$. Note that the natural frequency of (1) can be computed by the related autonomous system by setting $A = 0,$ which may change with the dynamical behaviors [33]. For example, when the trajectory oscillates around a focus, the natural frequency may be defined by the imaginary parts of the conjugate eigenvalues related to the equilibrium point, while when the trajectory oscillates according to a limit cycle, the corresponding frequency can be regarded as the natural frequency.

In the following, we will use the proposed method to investigate the mechanism of the dynamical evolution of the system, and reveal the influence of multi-stability on the bursting attractors. We first turn to the bifurcation analysis of the fast subsystem, i. e., the generalized autonomous system.

IV. BIFURCATION OF THE GENERALIZED AUTONOMOUS SYSTEM

Since the exciting frequency $\varepsilon\Omega$ is far less than the natural frequency, denoted by ω_N, the whole exciting term w can be regarded as a slow-varying bifurcation parameter, resulting in a generalized autonomous system, expressed also in the form (10).

The critical manifold can then be expressed by

$$-y - yz = 0,$$
$$x + ay + w = 0,$$
$$b + z(hx^2 - c) = 0,$$

(11)

corresponding to the equilibrium points of the fast subsystem. Obviously, two types of equilibrium points can be observed. The first type of the equilibrium point can be expressed as $E_0(x, y, z) = [-w, 0, b/(-hw^2 + c)],$ the stability of which can be determined by the related characteristic equation, written as

$$\lambda^3 + a_2\lambda^2 + a_1\lambda + a_0 = 0,$$

(12)

with

$$a_0 = -hw^2 b/(-hw^2 + c) - hw^2 + cb/(-hw^2 + c) + c,$$
$$a_1 = ahw^2 - ac + b/(-hw^2 + c) + 1,$$
$$a_2 = -hw^2 - a + c,$$

(13)

E_0 is stable when $a_0 > 0, a_2 > 0$ and $a_0 - a_1 a_2 > 0.$ It may lose the stability on two sets, one of which can be expressed by

$$\textbf{FB:}\ -hw^2 b/(-hw^2 + c) - hw^2 + cb/(-hw^2 + c) + c = 0,$$

(14)

with $a_2 > 0, a_0 - a_1 a_2 > 0,$ leading the jumping phenomenon between different equilibrium points via fold bifurcation, while the other of which can be defined by

$$\textbf{HB:}\quad \begin{aligned} & h^3w^6 + ah^2w^4 - 3ch^2w^4 - 2achw^2 + 3c^2hw^2 \\ & + ac^2 - c^3 + hw^2 - b - c = 0, (a_0 > 0, a_2 > 0), \end{aligned}$$

(15)

resulting in limit cycle via Hopf bifurcation.

The other type of equilibrium point can be expressed as $E_\pm(x,y,z) = [\pm\sqrt{(b+c)/h}, -w/a \mp \sqrt{(b+c)/h}/a, -1)$, the properties of which can be determined by the related eigenvalues defined by

$$(\lambda - a)[\lambda(b-\lambda)a - 2b - 2c \mp 2w\sqrt{h(b+c)}] = 0,$$

(16)

respectively. Obviously, for $a > 0$, or $b > 0$, $E_\pm$ are of saddle-type. When $a < 0$ and $b < 0$, E_+ is stable for $2w\sqrt{h(b+c)} + 2b + 2c < 0$, while E_- is stable for $2w\sqrt{h(b+c)} - 2b - 2c > 0$. Fold bifurcation may appear on the sets

$$\textbf{FB}_\pm \quad : \quad \pm 2w\sqrt{h(b+c)} + 2b + 2c = 0, (a < 0, b < 0),$$

(17)

possibly resulting in the jumping between different equilibrium points, while Hopf bifurcation may occur on the sets

$$\textbf{HB}_+: \quad b = 0, (a_0 < 0, 2w\sqrt{h(b+c)} + 2b + 2c > 0),$$

(18)

$$\textbf{HB}_-: b = 0, (a_0 < 0, 2w\sqrt{h(b+c)} - 2b - 2c > 0),$$

leading to periodic oscillations around $E_\pm$, with the frequencies approximated at $w_\pm^2 = 2w\sqrt{h(b+c)} \pm (2b+2c)$, respectively.

Remark: Note that the positions of the equilibrium points may change with the variation of the slow-varying parameter w, which forms equilibrium branches.

As an example, Fig.1 gives the equilibrium branches as well as the bifurcations on the (w,x) plane for the parameters fixed at $a = -0.1, b = -0.1, c = -0.1, h = -0.1$. The equilibrium branch E_0 is divided into three segments by the bifurcation points, corresponding to stable focus-type $E_0^{(1)}, E_0^{(3)}$ in which the segments $E_-^{(1)}, E_+^{(2)}$ are stable focus-type and the segments $E_-^{(2)}, E_+^{(1)}$ are unstable saddle-type, shown in Fig.1.

It can be found that when $w < w_- = -\sqrt{2}$, two stable foci E_0 and E_- coexist with the unstable saddle E_+, while at $w = w_-$, E_0 meets E_+, the fold bifurcation at FB_+ leads the alternations of the stabilities of the equilibrium points, which implies that E_0 becomes an unstable saddle point while E_+ changes to a stable focus. When w increases to $w = w_+ = +\sqrt{2}$, the saddle-type E_0 and the stable focus E_- collide, yielding fold bifurcation at FB_-, at which E_0 changes to a stable focus, while E_- becomes an unstable saddle.

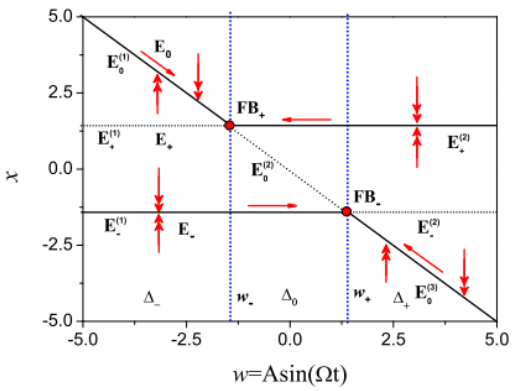

Figure 1: Equilibrium branches and bifurcations of the generalized autonomous system on the (w,x) plane double arrows indicate the direction of the fast flow and single arrows that of the slow flow.

Therefore, for the parameters fixed above, the slow-varying parameter w can be divided into three regions by the two fold bifurcation points, denoted by Δ_- with $w \in (-\infty, w_-)$, Δ_0 with $w \in (w_-, w_+)$ and Δ_+ with $w \in (w_+, +\infty)$, in which different types of equilibrium branches can be observed.

It is found that, when $w \in \Delta_\pm$ or $w \in \Delta_0$, there always one saddle and two stable equilibrium points with different attracting basins. The multi-stability may influence the dynamical behaviors of the full system, since the trajectory may visit different attracting basins under the effect of the fast and slow manifolds.

Obviously, for a fixed exciting amplitude A, the slow-varying parameter w may change between $-A$ and $+A$, i. e, $w \in [-A, +A]$, implying that the value of the exciting amplitude A determines the extreme values of w. Therefore, in the following, we focus on the evolution of the system with the increase of the exciting amplitude to explore the influence of the branches and their bifurcations of the fast subsystem on the dynamical behaviors of the full system.

V. DYNAMICAL EVOLUTION

To explore the slow-fast behaviors caused by the two scales in the frequency domain, here we fix the exciting frequency at 0.01 with parameters at $\varepsilon = 0.01, \Omega = 1.0$, which is far smaller than the natural frequency, while the other parameters are taken at the values described above. All the numerical results in the following are obtained by the variable step size Runge-Kutta method with the initial step at 0.001. To demonstrate the validity of the numerical simulations, different initial conditions for the step and the state variables are taken, while the constant step Runge-Kutta method is introduced to check the results.

For $A < \sqrt{2}$, no bifurcation occurs on the equilibrium branches of the generalized autonomous system. The state variables x and z settle down to the constant values at $x = \pm\sqrt{2}, z = -1$ with different initial values, respectively, while $y = \pm 5\sqrt{2} + A[\sin(0.01t)/0.2005 - \cos(0.01t)/4.01]$, which can be demonstrated by numerical simulations.

5.1 Two coexisted asymmetric periodic fold/fold bursting attractors

When A increases to $A > \sqrt{2}$, fold bifurcations at the two points $FB_\pm$ may influence the structure of the attractors. However, since both the two fold bifurcation points $FB_\pm$ connects the stable segment and unstable segment of $E_\pm$, delay of the bifurcation exists because of the slow passage effect. Numerical simulations reveal that when A increases to $A = 1.8225$, the influence of the fold bifurcations on the dynamics appears, which implies for $A \in (0.0, 1.8225)$, the trajectory moves with $(x, y, z) = (\pm\sqrt{2}, \pm 5\sqrt{2} + A[\sin(0.01t)/0.2005 - \cos(0.01t)/4.01], -1)$. When $A > 1.8225$, two coexisted bursting attractors appear, shown in Fig.2 for $A = 3.50$. Obviously, the two coexisted attractors are symmetric to each other, caused by the symmetry of the vector field. Furthermore, it can also be found that the trajectories of both the two attractors may oscillate around two types of equilibrium points, respectively.

To reveal the mechanism of the bursting oscillations, we turn to the transformed phase portrait on the (w, x) plane, together with the equilibrium branches and the related time history, shown in Fig.3. The trajectory alternates between two segments, corresponding to the large-amplitude

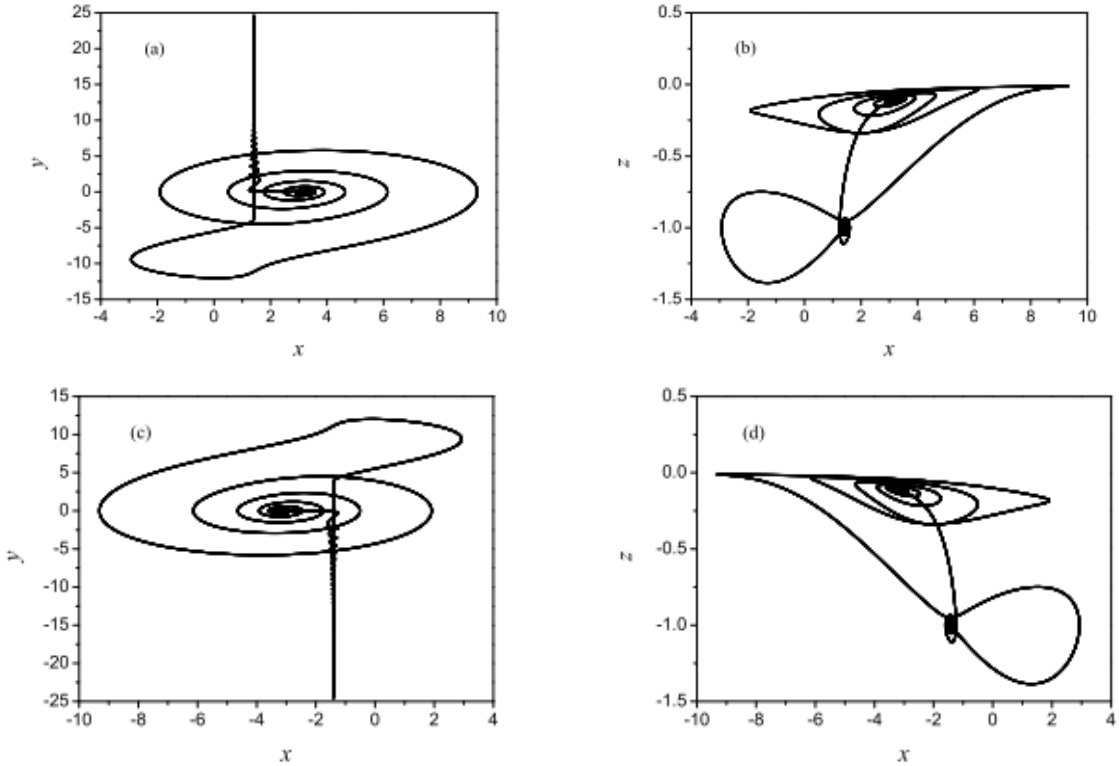

Figure 2: Two coexisted bursting attractors for $A = 3.50$. (a) The attractor on the (x, y) plane with the initial condition $(0.1,\ 0.1,\ 0.1)$ and the attractor on the (x, z) plane in (b); (c) The attractor on the (x, y) plane with the initial condition $(-0.1, -0.1, -0.1)$ and the attractor on the (x, z) plane in (d).

oscillations, denoted by SP, and small-amplitude oscillations or at rest, represented by QS, respectively, seeing Fig.3.

Assuming the trajectory starts at the point P_1, at which the slow-varying parameter w takes its minimum value with $w = -3.50$, it moves almost strictly along the stable equilibrium branch E_0, behaving in quiescent state QS. When the trajectory arrives at the point FB_+, it turns to move along the stable equilibrium branch E_+. Small-amplitude oscillations take place since the fold bifurcation causes the trajectory to move according to two different types of equilibrium branches. With the increase of w, the trajectory settles down to E_+ and moves almost strictly along E_+ until it arrives at the point P_2 at which w reaches its maximum value with $w = +3.50$.

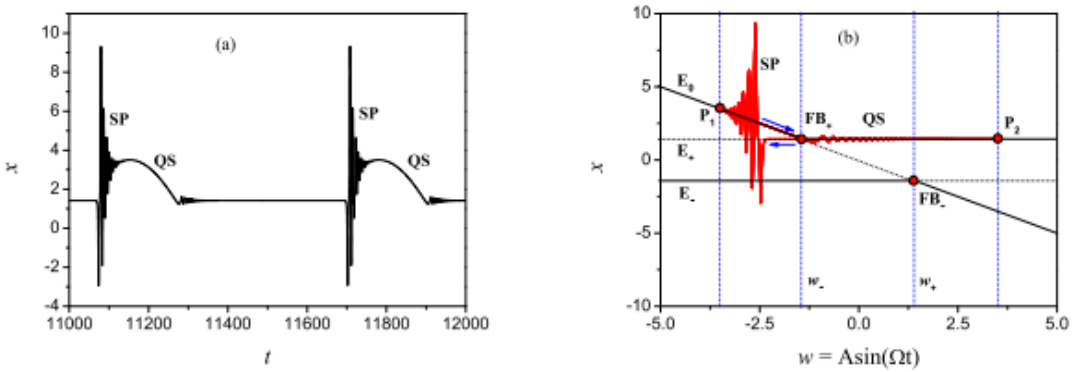

Figure 3: The structure of the attractor in Fig.2a. (a) The related time history of x; (b) Overlap of the transformed phase portrait and the equilibrium branches on the (w, x) plane.

The trajectory then turns to the left since w decreases with the increase of time, which still moves almost strictly along E_+. Because of the slow passage effect, when the trajectory reaches the point FB_+, it passes across the bifurcation point and turns to move almost strictly along the unstable equilibrium branch E_+ until the influence of the fold bifurcation appears. The trajectory then tries to approach the stable equilibrium branch E_0. However, since at the time the trajectory does not exactly locate on the equilibrium branch E_0, large-amplitude oscillations in spiking state SP occur, caused by the transient process of the trajectory from the current location to the stable focus-type branch.

The amplitudes of the oscillations decrease gradually and the trajectory finally settles down to E_0. When the trajectory arrives at the starting point P_1 on E_0, one period of the bursting oscillations is finished. It can be found the fold bifurcations cause the alternations between QSs and SPs on the trajectory. Therefore, the type of bursting attractor can be called asymmetric periodic fold/fold bursting oscillations.

Remark: The frequency of the repetitive spiking oscillations can be approximated by the imaginary parts of conjugate complex eigenvalues of the equilibrium point on the focus-type equilibrium branch E_0, which may change slowly with the variation of w From the related time history in Fig.3a, the frequency of the spiking oscillations can be approximated at 0.8925, which agrees well with the theoretical result at 0.8869, computed from the imaginary parts of the eigenvalues of the related equilibrium point.

5.2 Symmetric periodic fold/fold/fold/fold bursting oscillations

With the increase of the exciting amplitude, the two asymmetric attractors expand in the phase space, which may interact with each other to form an enlarged symmetric bursting attractor. Numerical simulations reveal that when $A = 5.0478$, a new type of symmetric bursting attractor appears, the trajectory of which may visit the two original asymmetric attractors in turn, seeing the attractor in Fig.4 for $A = 5.50$.

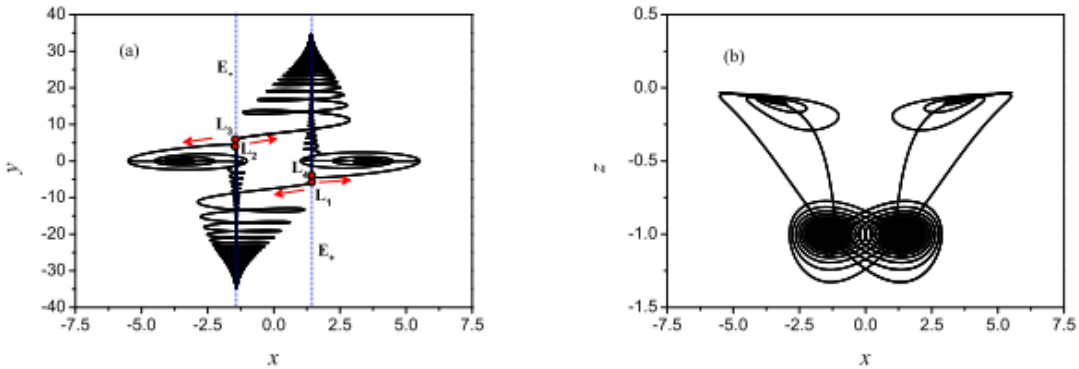

Figure 4: Symmetric bursting attractor for $A = 5.50$. (a) Phase portrait on the (x, y) plane; (b) Phase portrait on the (x, z) plane.

From the phase portrait of the attractor on the (x, y) plane in Fig.4a, one may find that two jumping phenomena occur for the trajectory moving almost strictly along the two equilibrium branches $E_\pm$ of the generalized autonomous system. For example, the trajectory along E_+ may jump to E_- at the point L_1 or jump to E_0 at the point L_4, seeing Fig.4a, while the trajectories of the two asymmetric attractors may jump only between $E_\pm$ and E_0, respectively.

Remark: With the increase of the exciting amplitude A, the inertia of the movement almost strictly along the two equilibrium branches $E_\pm$ increases so that the trajectory may visit both the two attracting basins of the associated stable equilibrium branches of the generalized autonomous system, causing the collision of the two asymmetric attractors to form an enlarged bursting attractor.

We now turn to the time history of x, presented in Fig.5, from which one may find that the trajectory can be divided into 8 segments, corresponding to four quiescent states $QS_i (i = 1, 2, 3, 4)$ and four spiking states $SP_i (i = 1, 2, 3, 4)$, respectively. Though there exist oscillations in the stages of QS_1 and QS_3, which are caused by the jumping between $E_\pm$ and E_0, since the jumping phenomena occur at the intersection points of the equilibrium branches, the amplitudes of the oscillations are very small.

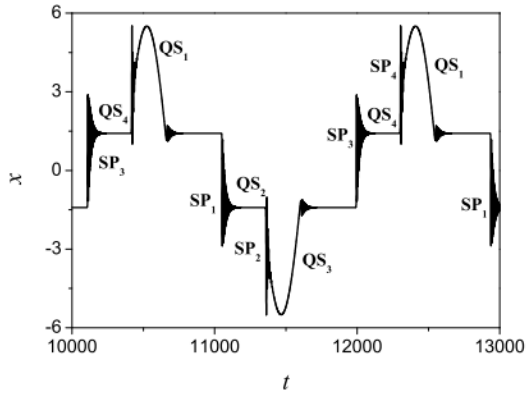

Figure 5: Time history of x for $A = 5.50$.

To reveal the mechanism of the bursting oscillations, we also turn to the overlap of the transformed phase portrait and the equilibrium branches on the (w, x) plane, plotted in Fig.6.

Assuming the trajectory starts at the point P_1 with $w = -5.50$, it moves almost strictly along the stable equilibrium branch E_0, behaving in quiescent state QS_1, until it arrives at the point FB_+. Fold bifurcation occurs, causing the trajectory to turns to move along E_+ with small-amplitude oscillations. The amplitudes of the oscillations gradually decrease and the trajectory finally settles down to E_+. When the trajectory reaches the point P_3 with the maximum of $w = +5.50$, it turns to left, moving almost strictly along E_+ .

The trajectory passes across the fold bifurcation point FB_+ , and then moves along the unstable segment of E_+, until it arrives at the point L_1, at which the effect of fold bifurcation occurs, seeing in Fig.6. The trajectory then jumps to the stable equilibrium branch E_- , yielding large-amplitude oscillations SP_1, the amplitudes of which decrease gradually, causing the trajectory to settle down to E_- at the point P_4 with $w = -5.50$.

The trajectory then turns to the right and moves almost strictly along E_- , passing across the point FB_- and appearing in quiescent state QS_2. When the trajectory arrives at the point L_2, the influence of the fold bifurcation occurs, causing the trajectory to jump to E_0, resulting in large-amplitude oscillations SP_2. The trajectory finally settles down to E_0 and moves almost strictly along E_0, behaving in quiescent state QS_3. Small-amplitude oscillations take place at the interaction point of E_0 and E_-, because of the fold bifurcation at the point FB_-. The trajectory then approaches the stable equilibrium branch E_- to the point P_4, then it turns to the right, moving almost strictly along E_-, passing across the fold bifurcation point FB_-. When the trajectory arrives at the point L_3, the fold bifurcation may cause the trajectory to jump to E_+, resulting in spiking oscillations SP_3. The amplitudes of the oscillations decrease gradually and the trajectory tries to settle down to E_+. When the trajectory reaches the point P_3, it turns to the left, moving almost strictly along E_+ passing across the fold bifurcation point FB_+ .

When the trajectory arrives at the point L_4, it approaches stable E_0 via fold bifurcation, leading to spiking oscillations SP_4. The trajectory tries to settle down to E_0 with gradual decrease of the oscillating amplitudes. Once the trajectory arrives at the starting point P_1, one period of the bursting oscillations is finished.

It can be found that four fold bifurcations take place, resulting in the transitions between the QS states and SP states during each period of the bursting oscillations. Therefore, the type of movement can be called symmetric periodic fold/fold/fold/fold bursting oscillations.

Furthermore, it can be found that the period of both the asymmetric bursting attractors is equal to that of the external excitation, while the period of the enlarged symmetric bursting oscillations is three times the period of the excitation.

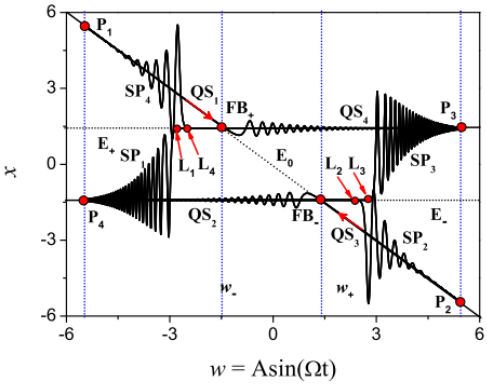

Figure 6: Overlap of the transformed phase portrait and the equilibrium branches as well as the related bifurcations on the (w, x) plane.

5.3 Symmetric breaking bifurcation to the bursting attractor

When the exciting amplitude increases to $A = 5.9482$, the symmetric bursting attractor splits into two coexisted asymmetric attractors, seeing one of which for $A = 5.95$ in Fig.7. The structure of the attractor is the same as that in Fig.3, while the quiescent state QS from the point P_2 along E_+ may pass across the point FB_+, implying the increase of the exciting amplitude may cause more delay of the influence of the bifurcation because of the increase of the inertia of the movement along the related equilibrium branch. Furthermore, the variation range of y along $x = \pm\sqrt{2}$ increases rapidly with the increase of A, seeing Fig.7a.

The structures of the pair of bursting attractors may qualitatively change when A increases to $A = 5.9993$, seeing the two coexisted asymmetric attractors in Fig.8 for $A = 6.0$.

Besides the two equilibrium points $E_\pm$, the trajectories of the two attractors may oscillate around the other equilibrium point E_0 with $x > 0$ or $x < 0$, respectively.

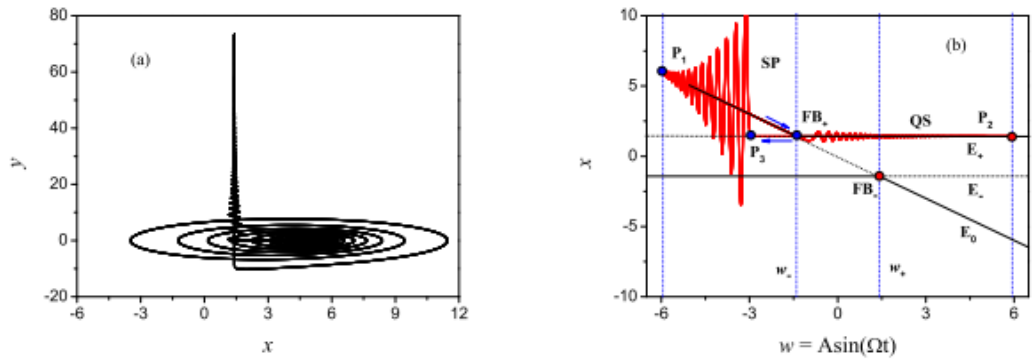

Figure 7: Bursting attractor for $A = 5.95$. (a) Phase portrait on the (x, y) plane; (b) Overlap of the transformed phase portrait and the equilibrium branches as well as the related bifurcations on the (w, x) plane.

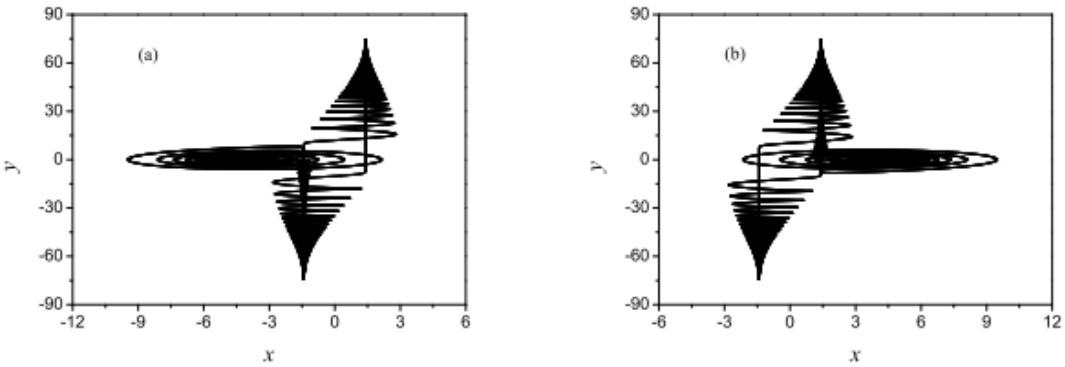

Figure 8: Two coexisted bursting attractors for $A = 6.0$ in (a) with the initial condition $(x, y, z) = (0.1, 0.1, 0.1)$ and in (b) with the initial condition $(x, y, z) = (-0.1, -0.1, -0.1)$.

Now we focus on the attractor in Fig.8a, the related time history of x and the transformed phase portrait on the (w, x) plane are plotted in Fig.9. From Fig.9a, it can be found that the trajectory of a period can be approximately divided into six segments, corresponding to three quiescent states and three spiking states, denoted by QS_i and SP_i with $i = 1, 2, 3,$ respectively. Note that during the segment QS_1, small-amplitude oscillations appear during two rest states along two different equilibrium branches, respectively.

For the trajectory starting from the point P_1 with $w = -6.0$, it moves almost strictly along the stable equilibrium branch E_-, passing across the bifurcation point FB_-, behaving in quiescent state QS_1 until it arrives at the point L_1, seeing Fig.9b. The effect of fold bifurcation at FB_- appears, causing the trajectory jumps to the stable equilibrium branch E_+, resulting in spiking oscillations SP_1, seeing Fig.9c. The amplitudes of the oscillations decrease gradually and finally the trajectory settles down to E_+. When the trajectory reaches the point P_2 with $w = +6.0$, it turns to the left with the evolution of time. The trajectory moves almost strictly along E_+ in quiescent state QS_2, passing across the bifurcation point FB_+, until it arrives at the point L_2. The effect of fold bifurcation causes the trajectory to jump to stable E_-, resulting in repetitive spiking oscillations SP_2, shown in Fig.9d.

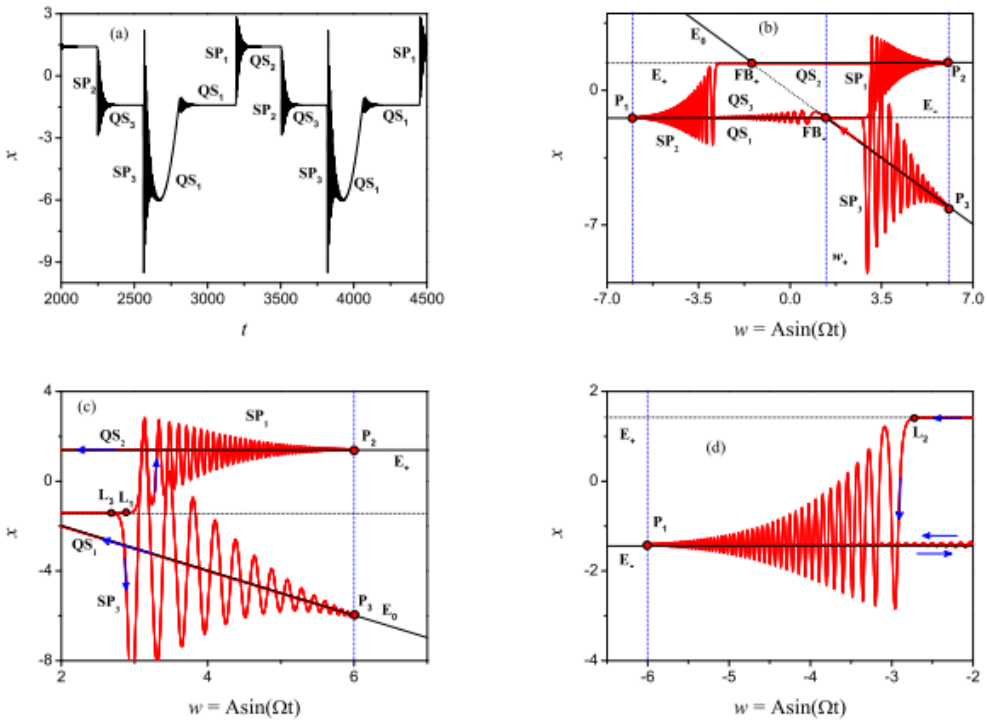

Figure 9: Bursting attractor in Fig.8a. (a) Time history of x; (b) Overlap of the transformed phase portrait and the equilibrium branches as well as the related bifurcations on the (w, x) plane with locally enlarged parts in (c) and (d).

When the trajectory moves to the point P_1 with gradual decrease of the oscillating amplitudes, it turns to the right, moving almost strictly along E_- in quiescent state QS_3 until it reaches the point L_3. Fold bifurcation causes the trajectory to the equilibrium branch E_0, leading to spiking oscillations SP_3. The trajectory may gradually settle down to E_0, with further increase of time, until it reaches the point P_3. Then the trajectory moves almost along E_0 towards the point FB_- in quiescent state QS_1. The fold bifurcation at the point FB_- causes the trajectory to turn to move along E_-, leading to small-amplitude oscillations, which may quickly disappear with the increase of time.

When the trajectory moving along E_- arrives at the starting point P_1, one period of the bursting oscillations is finished. The period of the oscillations can be computed exactly at $4\pi / \Omega$, which is two times the

period of the external excitation. Furthermore, the type of oscillations can be called asymmetric periodic 6-fold bursting attractor, since only fold bifurcations take place at the transition between QSs and SPs.

With the increase of the exciting amplitude, both the two asymmetric attractors may evolve to a symmetric bursting attractor, seeing Fig.10. Comparing the two cases with $A = 6.0$ and $A = 6.045$, respectively, one may find that for $A = 6.0$, the part D_1 in Fig.10a along with the stable equilibrium branch $E_0^{(1)}$ or $E_0^{(3)}$ in Fig.1 preserves, implying the trajectory from $E_0^{(1)}$ or $E_0^{(3)}$ may return to the same equilibrium branch. However, for $A = 6.045$, the part D_1 in Fig.10b and Fig.10d corresponds to the transient, which may finally disappear, leading to the steady time history of x in Fig.10c, which can also be demonstrated by the phase portrait presented in Fig.11a.

It can also be understood that for $A = 6.0$, the trajectory may visit the attracting basins related to stable $E_0^{(1)}$, $E_-^{(1)}E_+^{(2)}$, or those associated with $E_0^{(3)}$, $E_-^{(1)}E_+^{(2)}$, respectively, while for $A = 6.045$, the trajectory only alternates between stable segments of $E_\pm$.

Now we turn to the steady state of the attractor, of which the related phase portrait on the (x, y) plane and the transformed phase portrait on the (w, x) plane are given in Fig.11. From the phase portrait in Fig.11a, one may find that the trajectory oscillating down to one equilibrium branch of $E_\pm$, may jump to approach the other equilibrium branch of $E_\pm$ via fold bifurcations.

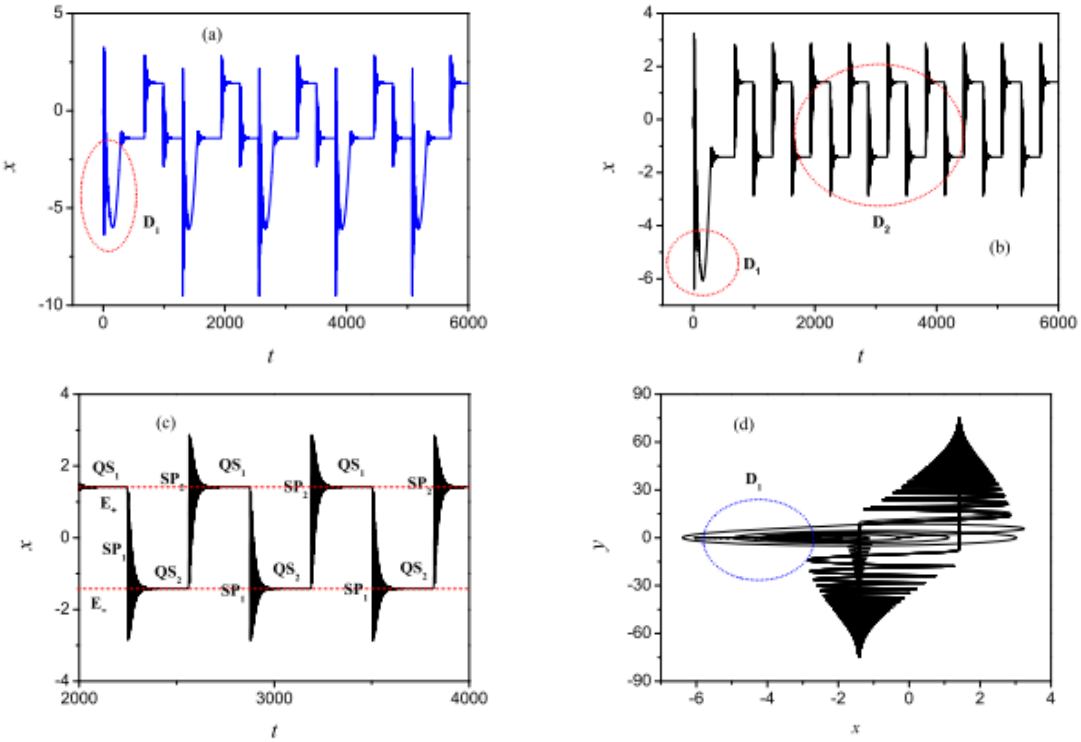

Figure 10: (a) Time history of x for $A = 6.0$; (b) Time history of x for $A = 6.045$; (c) Steady part of the time history for $A = 6.045$; (d) Phase portrait on the (x, y) plane for $A = 6.045$.

The trajectory, starting from the point P_1 with $w = -6.045$, moves almost strictly along stable $E_-^{(1)}$,passing across the bifurcation point FB_-, and turns to move almost strictly along the unstable $E_-^{(2)}$ in quiescent state QS_1 because of the delay effect of the bifurcation. When the trajectory arrives at the point L_1, it jumps to stable $E_+^{(2)}$ via fold bifurcation, resulting in the repetitive spiking oscillations SP_1 around $E_+^{(2)}$. With the gradual decrease of the oscillating amplitude, the trajectory finally settles down to $E_+^{(2)}$ at the point P_2 with $w = +6.045$. Half period of the bursting oscillations is finished, while the other half period of the oscillations is omitted here for simplicity because of the symmetry. The type of oscillations can be called symmetric periodic fold/fold bursting attractor with the same period as that of the external excitation.

Further increase of the exciting amplitude may cause the bursting oscillations to alternate among those bursting attractors described above. Furthermore, the attractor may expand along the equilibrium branches on the

(w, x) plane, seeing Fig.12 for example. It can be found that the mechanism of the bursting is the same as that in Fig.6, while the structure of the attractor expands greatly in the phase space, causing the amplitudes of the spiking oscillations to increase dramatically.

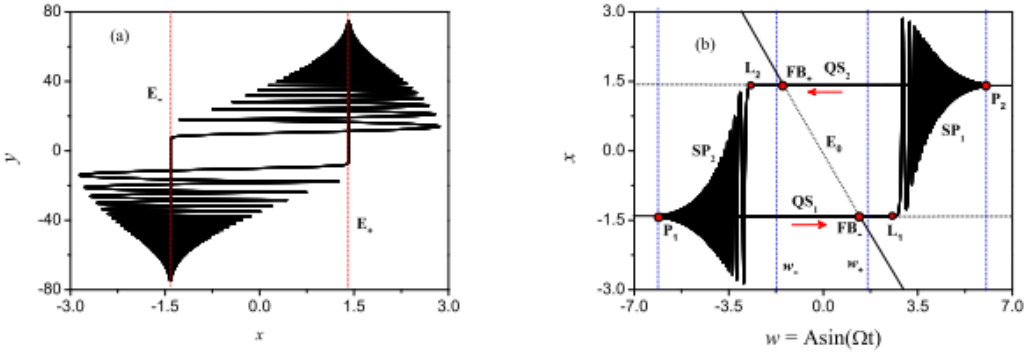

Figure 11: Symmetric bursting oscillations for $A = 6.045$. (a) Phase portrait on the (x, y) plane; (b) Overlap of the transformed phase portrait and the equilibrium branches.

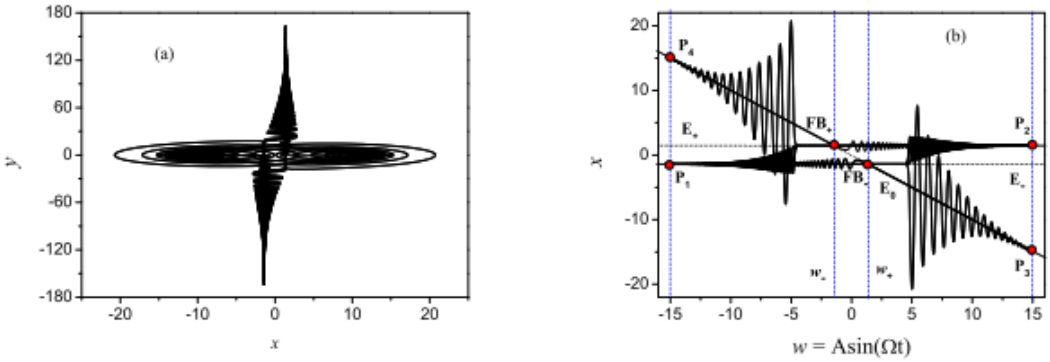

Figure 12: Symmetric bursting oscillations for $A = 15.0$. (a) Phase portrait on the (x, y) plane; (b) Overlap of the transformed phase portrait and the equilibrium branches.

In summary, for the generalized autonomous system, there exist multiple stable segments on the equilibrium branches. With the increase of the exciting amplitude, the bursting attractors may oscillate around different groups of these stable segments, which, therefore, results in different types of bursting attractors.

VI. CONCLUSIONS

When the exciting frequency is far less than the natural frequency, bursting oscillations may occur, the mechanism of which can be investigated by the proposed method. With the variation of the slow-varying parameter, defined by the whole exciting term, the multi-stability may cause coexisted stable equilibrium branches in the generalized autonomous system. The trajectory may visit different groups of the related attracting basins of the stable equilibrium branches, which may result in different forms of the bursting attractors. Furthermore, the dynamics may alternate between a symmetric attractor and a pair of coexisted asymmetric attractors with the variation of the exciting amplitude, depending on the particular attracting basins the trajectory visits.

ACKNOWLEDGMENTS

The work is supported by the National Natural Science Foundation of China (Grant Nos. 11632008,11872188, 11872189 and 11972173).

Declaration of conflicting interests

The authors declared no potential conflicts of interest with respect to the research, authorship, and/or publication of this article.

REFERENCES

[1]. K. D. Mease, Multiple time scales in nonlinear flight mechanics:diagnosis and modeling, Appl. Math. Computat, 164 (2005) 627-648.

[2]. A. Rasmussen, J. Wyller, J. O. Vik, Relaxation oscillations in spruceCbudworm interactions, Nonlinear Analysis: Real World Appl. 12 (2011) 304-319.

[3]. J. Guckenheimer, P. Holmes, Nonlinear Oscillations, Dynamical Systems and Bifurcations of Vector Fields, Springer-Verlag, New York, 1983.

[4]. A. L. Hodgkin, A. F. Huxley, A. F., A quantitative description of membrane current and application to conduction and excitation in nerve, J. Phys. 117 (1952) 500-544.

[5]. A. Surana, G. Haller, Ghost manifolds in slow-fast systems, with applications to unsteady fluid separation, Physica D 237 (2008) 1507-1529.
F. Verhulst, Singular perturbation methods for slow-fast dynamics, Nonlinear Dynamics 50 (2007) 747-753.

[6]. J. Shen, Z. Zhou, Fast-slow dynamics in first-order initial value problems with slowly varying parameters and application to a harvested logistic model, Communications in Nonlinear Science and Numerical Simulation 19 (2014) 2624-2631.

[7]. O. Decroly, A. Goldbeter, From simple to complex oscillatory behavior: analysis of bursting in a multiply regulated biochemical system, J. Theor. Biol. 124 (1987) 219-250.

[8]. Yu. A. Kuznetsov, Elements of Applied Bifurcation Theory, Springer, New York, 2004.

[9]. F. Takens, Constrained equations: A study of implicit differential equations and their discontinuous solutions, Structural Stability, the Theory of Catastrophes and Applications in the Science, Springer-Verlag, New York, 1976.

[10]. M. Desroches, J. Guckenheimer, B. Krauskopf, C. Kuehn, H. M. Osinga, M. Wechselberger, Mixed-mode oscillations with multiple time scales, SIAM Review 54 (2012) 211-288.

[11]. N. Fenichel, Geometric singular perturbation theory for ordinary differential equations, J. Differential Equations, 31 (1979) 53-98.

[12]. S. J. Fraser, The steady state and equilibrium approximations: a geometrical picture, J. Chem. Phys. 88 (1988) 4732-4738.

[13]. J. Guckenheimer, R. Harris-Warrick, J. Peck, A. R. Willms, Bifurcation, bursting, and spiking frequency adaptation, J. Comput. Neurosci. 4 (1997) 257-277.

[14]. J. Rinzel, G. Huguet, Nonlinear Dynamics of Neuronal Excitability, Oscillations, and Coincidence Detection, Communications on Pure and Applied Mathematics 66 (2013) 1464-1494.

[15]. C. Wang, X. Zhang, Canards, heteroclinic and homoclinic orbits for a slow-fast predator-prey model of generalized Holling type III, J. Differential Equations 65 (2019) 3397-3441.

[16]. S. Ai, S. Sadhu, The entry-exit theorem and relaxation oscillations in slow-fast planar systems, J. Differential Equations 268 (2020) 7220-7249.

[17]. M. Aggarwal, N. Cogan, R. Bertram, Where to look and how to look: Combining global sensitivity analysis with fast/slow analysis to study multi-timescale oscillations, Math. Biosciences 314 (2019) 1-12.

[18]. J. Guckenheimer, C. Kuehn, Computing slow manifold of a saddle type, SIAM J. Appl. Dyn. Syst. 8 (2009) 854-879.

[19]. R. Bertram, J. E. Rubin, Multi-timescale systems and fast-slow analysis, Math. Biosci. 287 (2017) pp. 105-121.

[20]. E. M. Izhikevich, Neural excitability, spiking and Bursting, Int. J. Bifur. Chaos 10 (2000) 1171- 1266.

[21]. J. Rinzel, Discussion: Electrical excitability of cells, theory and experiment: Review of the Hodgkin-Huxley foundation and an update, Bull. Math. Bio. 52 (1990) 5-23.

[22]. W. Teka, J. Tabak, R. Bertram, The relationship between two fast/slow analysis techniques for bursting oscillations, Chaos: An Interdisciplinary Journal of Nonlinear Science 22 (2012) 043117.

[23]. X. Wang, W. Li, Y. Wu, Novel results for a class of singular perturbed slow-fast system, Applied Mathematics & Computation, 225 (2013) 795-806.

[24]. Z. D. Zhang, Y. Y. Li, Q. S. Bi, Routes to bursting in a periodically driven oscillator, Physics Letters A 377 (2013) 975-980.

[25]. Q. S. Bi, S. L. Li, J. Kurths, Z. D. Zhang, The mechanism of bursting oscillations with different codimensional bifurcations and nonlinear structures, Nonlinear Dynamics 85 (2016) 1-13.

[26]. Q. S. Bi, R. Ma, Z. D. Zhang, Bifurcation mechanism of the bursting oscillations in periodically excited dynamical system with two time scales, Nonlinear Dynamics 79 (2015) 101-110.

[27]. E. N. Lorenz, Deterministic nonperiodic flows, J. Atmos. Sci. 20 (1963) 130-141.

[28]. G. Chen, T. Ueta, Yet another chaotic attractor, Int. J. Bifurcation Chaos 9 (1999) 1465-1466.

[29]. J. C Sprott, Simplest chaotic flows with involutional symmetries, Int. J. Bifurcation Chaos 24 (2014) 1450009.

[30]. N. V. Kuznetsov, T. N. Mokaev, P. A. Vasilyev, Numerical justification of Leonov conjecture on Lyapunov dimension of Rossler attractor, Commun. Nonlinear Sci. Numer. Simulat. 19 (2014) 1027-1034.

[31]. R. B. Alstrom, S. Moreau, P. Marzocca, K. Bollt, Nonlinear characterization of a Rossler system under periodic closed-loop control via time-frequency and bispectral analysis, Mech. Systems Signal Processing 99 (2018) 267-585.

[32]. X. Han, Q. S. Bi, P. Ji, J. Kurths, Fast-slow analysis for parametrically and externally excited systems with two slow rationally related excitation frequencies, Phys. Rev. E 92 (2015) 012911.

Yandan Jiang, et. al. "Slow-fast oscillations in a periodically excited symmetric chaotic oscillator with multiple time scales." *International Journal of Modern Engineering Research (IJMER),* vol. 11(01), 2021, pp 24-37.